

Relativistic effects in nonrelativistic ionization

H. R. Reiss

Max Born Institute, 12489 Berlin, Germany, and American University, Washington, D.C. 20016-8058, USA

(Received 11 December 2012; published 27 March 2013)

Radiation pressure effects recently observed by Smeenck *et al.* [C. Smeenck, L. Arissian, B. Zhou, A. Mysyrowicz, D. M. Villeneuve, A. Staudte, and P. B. Corkum, *Phys. Rev. Lett.* **106**, 193002 (2011)] in atomic ionization by circularly polarized light are readily explained by the relativistic strong-field approximation (RSFA). The physical picture that emerges is determined by linear and angular momentum properties of the photons required for ionization, and it is largely independent of the atom being ionized. Radiation pressure follows from linear momenta carried by photons, and the angular momenta of the photons require the photoelectron to be in a circular orbit around the remnant ion. Two special features of the Smeenck *et al.* experiments are highlighted by the analysis. One is that this is the first verification of true relativistic effects in ionization. The other is that the circular trajectory picture from the RSFA analysis directly contradicts the physical picture that emerges from the length gauge. This is an exceptionally striking example of gauge-dependent differences in physical interpretations. Nevertheless, the distribution of momentum found by the Smeenck *et al.* experiments is accurately predicted by the RSFA. Results herein provide a universal theory to which the analysis of Titi and Drake [A. S. Titi and G. W. F. Drake, *Phys. Rev. A* **85**, 041404(R) (2012)] represents an approximation. The physical properties of ionization by circularly polarized light also cast doubt on some predictions of rescattering theory.

DOI: [10.1103/PhysRevA.87.033421](https://doi.org/10.1103/PhysRevA.87.033421)

PACS number(s): 32.80.Rm, 32.80.Wr, 31.30.J-

I. INTRODUCTION

Recent experiments by Smeenck *et al.* [1] (henceforth referred to as Smeenck) on atomic ionization by a circularly polarized laser beam showed slight departures from the symmetry expected in nonrelativistic experiments. This asymmetry was recognized as due to radiation pressure, which was assessed with a classical model. The same experiments were analyzed by Titi and Drake [2] (referred to henceforth as T&D) using a quantum approximation to extend nonrelativistic results. In the present work it is shown that a theory that is entirely relativistic from the outset provides a simple, complete, and physically transparent picture of the novel aspects of the Smeenck measurements. The analyses done by Smeenck and by T&D are relatively complicated. The analysis can be directly and accurately done by using the relativistic strong-field approximation (RSFA) method [3]. Another advantage of the RSFA is that all observed phenomena are placed in a universal context, providing a simple explanation of photoelectron properties as direct consequences of the linear and angular momenta of the photons that participate in the ionization.

Two unusual features characterize the analysis of the Smeenck experiments. One is that the Smeenck work provides the first realization of true relativistic effects long predicted, but not previously observed. The other is that the physical picture that emerges from the length gauge analysis done by Smeenck contrasts strongly with the physical interpretation provided by the Coulomb gauge, even when there is agreement in the predicted momentum distributions.

The RSFA, elucidated more than 20 years ago but not previously tested, uses the Dirac-Volkov wave function for the final state, and a solution of the Dirac equation for atomic hydrogen in the initial bound state, incorporated into a Dirac-relativistic *S*-matrix formalism. Application of the RSFA to laboratory experience has been hindered heretofore by the high intensities perceived as necessary to exhibit relativistic effects. Such high intensities would cause saturation of the ionization

process in the rising phase of a pulsed laser before relativistic behavior would set in. The obvious way to circumvent that problem would be to use a laser of very low frequency. That will occur eventually, but the exceptional sensitivity of the Smeenck experiments have provided an alternative solution by allowing observation of relativistic effects in an otherwise nonrelativistic environment. The experiments to be analyzed employ circular polarization so that, for high intensities, the photoelectron spectrum peaks at an energy approximately that of the ponderomotive energy U_p . This makes the RSFA very accurate, since the only approximation made is that the photoelectron interaction with the laser field (measured by U_p) should be greater than the neglected Coulomb interaction of the remnant ion for the photoelectron (measured by the binding energy E_B). This condition is well-satisfied for all but the lowest intensity portions of the experimental results.

The T&D approximation for the distribution of momentum components parallel to the propagation direction $p_{||}$ is a nearly exact match to the fully relativistic predictions of the RSFA. In the original RSFA paper [3], a very simple and universal expression was found that provides an immediate explanation for the vital result $p_{||} = U_p/c$. The result, also found by T&D, is in good agreement with the experiments and has the unusual feature that it depends only on the frequency and intensity of the laser field, with no essential dependence on the properties of the atom being ionized.

Smeenck, in conflict with the RSFA, concludes that “the ponderomotive energy does not transfer any net momentum to the electron” [1]. Their analysis concludes that radiation pressure imparts $2U_p/c$ momentum to the photoelectron, of which U_p/c is subtracted by the effect of the intensity envelope of the pulsed laser beam. A striking contrast is that the classical analysis of Smeenck posits an initial velocity \mathbf{v} of the photoelectron that is parallel to the electric field direction, whereas the relativistic quantum analysis presented herein predicts an initial photoelectron velocity that arises from a circular motion around the residual ion and is thus

perpendicular to the electric field. This is a contrast in gauge-dependent physical interpretations rivaling that found by Lamb [4] in his strongly gauge-dependent calculation of the line-shape associated with a Lamb-shift calculation, a dilemma resolved by Fried [5].

The calculations reported here lead to the conclusion [6] that the photoelectron ionized by circularly polarized light enters into a circular orbit around the remnant ion rather than “walking away” from the ion as predicted by rescattering theory [7,8].

A general remark about the role of relativity in strong-field phenomena is appropriate here. In traditional atomic, molecular, and optical (AMO) physics, the Coulomb binding potential is the dominant feature, and relativistic effects exist as relatively small corrections to a basically nonrelativistic discipline. In the strong laser fields that are now available, the ponderomotive potential U_p can strongly dominate the binding energy E_B . When that is true, the fundamentally relativistic nature of the photon field becomes a centrally important feature of laboratory interactions, and it is conceptually perilous to overlook that basic fact. See Refs. [9–11] for further discussion.

II. QUALITATIVE PHOTON EFFECTS

Atomic ionization by a circularly polarized laser beam illustrates fundamental angular momentum properties of a photon. The angular momentum carried by a single circularly polarized photon is \hbar for *all* frequencies. For example, a far-infrared photon conveys as much angular momentum as does an energetic γ ray. In strong-field laser processes where many photons are absorbed in an ionization event, the angular momenta of circularly polarized photons are additive, thus making the transfer of angular momentum an important consideration at laser frequencies. Another aspect of this comparison is that the angular momentum of an individual photon is of the same order of magnitude as the electron spin or of changes in the orbital angular momentum quantum number of a bound electron.

The transfer of linear momentum by a photon is qualitatively different from the transfer of angular momentum. The ratio of the energy of a single photon $\hbar\omega$ to its momentum $\hbar\omega/c$ has the value c , whereas the same ratio for a nonrelativistic electron is $(mv^2/2)/mv = v/2$. That is, for comparable nonrelativistic energies, the photon is a very ineffective carrier of momentum as compared to an electron.

As applied to the Smeenk experiments, this explains why photon angular momentum plays a dominant role, whereas photon linear momentum, manifested as radiation pressure, requires a sensitive measurement technique to be observed.

III. PHOTOELECTRON MOMENTUM COMPONENTS

When an atomic electron is ionized by a strong, circularly polarized laser field, the final state is a photoelectron that possesses a kinetic energy equal to about the ponderomotive energy U_p of a free electron in the field. As mentioned above, the photoelectron also possesses the summed angular momentum of all the photons required to achieve ionization. For strong fields, where the ponderomotive potential of the free electron in the field is dominant over the binding energy of

the electron in the atom, the photoelectron must have absorbed approximately the energy and angular momentum of a number of photons equal to $2U_p/\hbar\omega$, where one factor of U_p represents the ponderomotive potential of the free electron in the laser field and the other is its kinetic energy. These conditions,

$$T \approx U_p, \quad L \approx 2U_p/\omega, \quad (1)$$

(where T is the kinetic energy, L is the angular momentum, and atomic units are used here and hereafter) replicate the classical kinetic energy and angular momentum of a free electron in a rotational motion centered on the initial neutral atom. Nonrelativistically, the plane of the circular motion perpendicular to the propagation direction of the field includes the ion; relativistically, the radiation pressure exerted by the laser field causes a displacement of the rotational pattern in the direction of propagation of the field. These conditions are sketched in Fig. 1, taken from Ref. [12]. As shown in Ref. [3], the angle of forward displacement θ_d with respect to the nonrelativistic plane of motion is

$$\theta_d = \arctan\left(\frac{1}{2}z_f^{1/2}\right), \quad (2)$$

$$z_f \equiv 2U_p/c^2 \Rightarrow \theta_d = \arctan\left[\frac{1}{c}(U_p/2)^{1/2}\right]. \quad (3)$$

The dimensionless parameter z_f in Eq. (3) is the ratio of twice the ponderomotive potential to the rest energy of the electron. It is ubiquitous in the theory of free electron processes in strong fields, albeit with many different notations. Figure 2 is a sample calculation with the RSFA, using parameters that produce an angular distribution resembling that of Fig. 1. The field conditions are unrealistically extreme, but are selected to show clearly the influence of radiation pressure. The radiation-pressure deflection angle of Eq. (2) is a kinematical prediction,

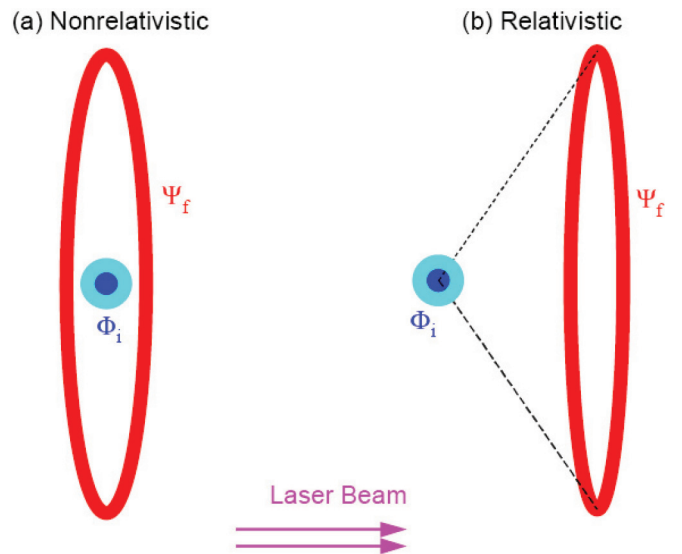


FIG. 1. (Color online) This figure illustrates the effect of radiation pressure on the path of a photoelectron ionized by circularly polarized light. The circular orbit is the result of the summed angular momenta of the photons required for ionization. The forward displacement of the plane of the orbit is the result of photon linear momenta. The figure is taken from Ref. [12].

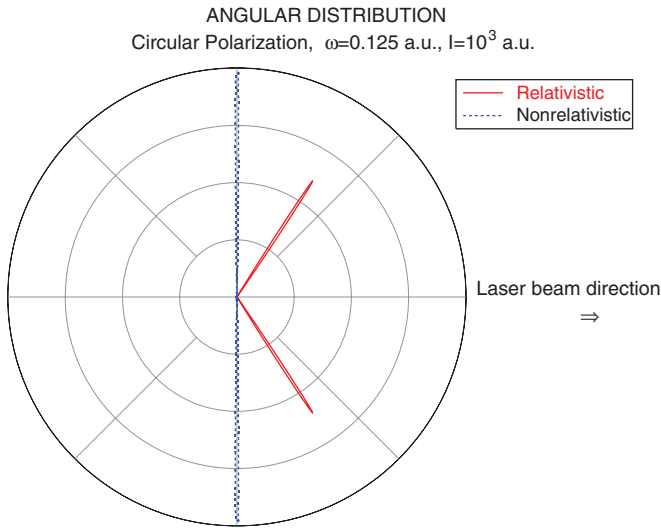


FIG. 2. (Color online) The angular distribution of photoelectrons predicted by an RSFA calculation, done with neither focal averaging nor saturation effects included. The peak of the angular distribution occurs at the angle given by Eq. (2). To illustrate an extreme effect of radiation pressure in order to mimic Fig. 1, the intensity is selected to be unrealistically high. The atom would be fully ionized at a much lower intensity.

but dynamical calculations with the RSFA produce exactly this angle.

The component of momentum p_{\parallel} parallel to the propagation direction of the laser field is related to the perpendicular component p_{\perp} by the relation

$$p_{\parallel} = p_{\perp} \tan \theta_d = p_{\perp} (U_p/2c^2)^{1/2}. \quad (4)$$

The perpendicular component of momentum can be approximated by the nonrelativistic expression $p_{\perp} \approx \sqrt{2T} \approx \sqrt{2U_p}$. This gives the component of momentum parallel to the direction of propagation as

$$p_{\parallel} = \frac{U_p}{c}. \quad (5)$$

A notable fact about Eq. (5) is that the parallel momentum is independent of the identity of the atom. The parallel momentum, using the connection to field intensity I and frequency ω given by $U_p = I/(2\omega)^2$, is

$$p_{\parallel} = \frac{I}{4\omega^2 c}. \quad (6)$$

This is plotted in Fig. 3(a) for the frequencies corresponding to wavelengths of 800 and 1400 nm employed in Refs. [1,2]. Figure 3(b), reproduced from Ref. [1], shows that the RSFA produces the same trends that are found in the experiments, keeping in mind that Eqs. (5) and (6) relate only to high intensities.

The components p_{\parallel} and p_{\perp} are defined with respect to the direction of propagation of the laser field. This means that p_{\perp} is actually an azimuthal component of the momentum of the photoelectron as it follows a circular trajectory about the original atom; the component p_{\parallel} is directly due to the influence of the “radiation pressure” that follows from the linear momenta of the absorbed photons. Both components of

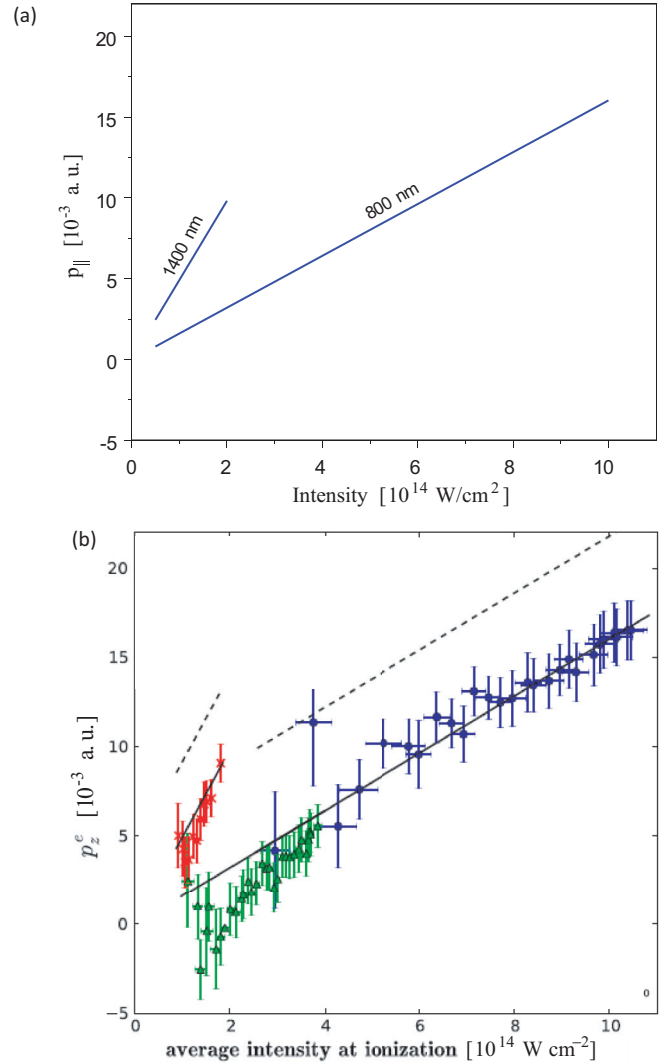


FIG. 3. (Color online) Components of momentum parallel to the propagation direction of a circularly polarized laser field depend primarily on the frequency and intensity of the laser field rather than on properties of the atom being ionized. Part (a) is the prediction of Eq. (5) or (6) for the two wavelengths employed by Smeenk. The lines shown closely replicate those found by the experiments. Figure 3(b) is taken from Ref. [1].

momentum represent cumulative contributions of the photons absorbed in order to ionize the atom. The parameters of the circular motion are classical. The center of rotation is fixed at the center of the atom, since the axis of rotation of a photoelectron is given by the intersection of the propagation vector \mathbf{k} with the location of the atom. The situation is graphically illustrated in Fig. 1, and the components of linear momentum are related to each other as shown in Eq. (4).

The parameters illustrated in Fig. 1 are clearly more dramatic than those that pertain to the Smeenk experiments. However, in all calculational experience with relativistic ionization by circularly polarized light, the simple geometrical considerations that led to the deflection angle (2) are exactly obeyed in the detailed dynamical calculations done with the RSFA. Some examples of the outcome of such calculations are given in Ref. [13], in Sec. 8 on “Relativistic Effects.”

In particular, Fig. 2.19 of Ref. [13] gives the angular distribution of photoelectrons from ionization of ground-state hydrogen by a field of frequency $\omega = 0.125$ a.u. at an intensity of 10^3 a.u. To make that figure more relevant to the present discussion, the rectangular coordinates are replaced by polar coordinates, the logarithmic scale of magnitude is replaced by a linear scale, and the direction of propagation of the field is reversed. The result is Fig. 2, representing conditions not unlike those shown in Fig. 1. The angle of dominant emission is given exactly by Eq. (2).

IV. PHOTOELECTRON MOMENTUM DISTRIBUTION

References [1,2] both present a figure showing the relative probability for values of the parallel momentum component p_{\parallel} (or p_z) for the case of ionization of neon ($E_B = 21.5645$ eV) by circularly polarized light at 800 nm and 8×10^{14} W/cm². The RSFA gives the analytical expression for the momentum distribution as

$$\frac{dW}{dp_{\parallel}} = \frac{4c^4}{\pi} z_f Z^5 \sum_{n=n_0}^{\infty} \frac{(u_A + u_B + u_C)}{(Z^2 + \rho^2)^4}, \quad (7)$$

where Z is the nuclear charge, z_f is defined in Eq. (3), and the quantities u_A , u_B , u_C , and ρ are defined in Ref. [3] by expressions that are too lengthy to warrant reproduction here. It is notable that dependence on Z is identical to that given in Eq. (13) of T&D [2] and so is the quantity in the denominator raised to the fourth power. This is quite interesting in view of the fact that the T&D expression is a correction to nonrelativistic results, whereas Eq. (7) is valid for fully relativistic conditions. A plot of the results of Eq. (7) is given in Fig. 4(a) for the same parameters as shown in the equivalent figures in Refs. [1,2]. Figure 4(b) is reproduced from Ref. [2] for comparison. The two parts of Fig. 4 are nearly identical.

The model of ionization by circularly polarized light as shown in Fig. 1 has support from other considerations. The momentum distribution for photoelectrons from ionization with circular polarization as given in the work of Bergues *et al.* [14] is shown here in Fig. 5. Although the authors seem not to have noticed it at the time (see Ref. [6]), the figure is clearly generated by a pattern of photoelectrons rotating around the remnant ion. Further evidence comes from a numerical calculation of the U matrix (giving the time evolution of an S matrix) for ground-state hydrogen ionized by a single-period Gaussian pulse of circularly polarized light [15]. The result of the calculation is that the quantum probability distribution of the atomic electron moves out to the classical radius of motion as the field strength increases. When the pulse recedes, most of the distribution returns to the bound state, except for an intensity-dependent deficit. It is that deficit that represents the ionization caused by the pulse. The end result of this short-pulse analysis is fully consistent with a long pulse giving rise to a photoelectron in a circular trajectory around the atom.

V. ROLE OF THE PONDEROMOTIVE POTENTIAL

The ponderomotive potential U_p is a fundamental property of plane-wave phenomena, of which laser fields are an

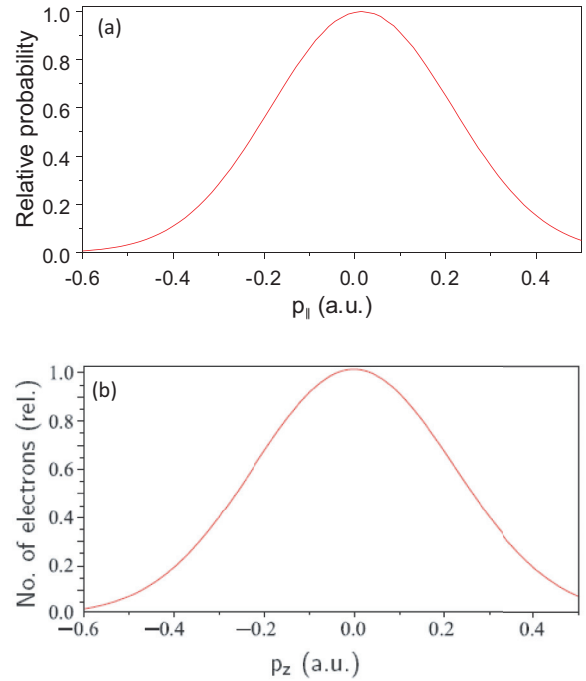


FIG. 4. (Color online) An explicit calculation of the distribution of momentum components parallel to the direction of propagation of a circularly polarized laser beam, done with the RSFA [3] for the case of neon ionized by a laser of 800 nm in wavelength and an intensity of 8×10^{14} W/cm² is shown in part (a) of the figure. The approximation due to T&D [2] produces the result shown in part (b) of the figure, which is taken from Ref. [2]. The two calculations give nearly identical results, showing a slight tilt towards the beam propagation direction.

important example. It can be written in various ways, but when expressed in terms of the square of the vector potential, it can be shown to be both Lorentz invariant and gauge invariant [16,17]. This poses a problem for the length gauge, which has no vector potential. That conundrum arises from the fact that a plane-wave field (e.g., a laser field) is a vector field, so that it can never be fully described by a scalar potential alone. This is a subtle subject that is treated at length elsewhere

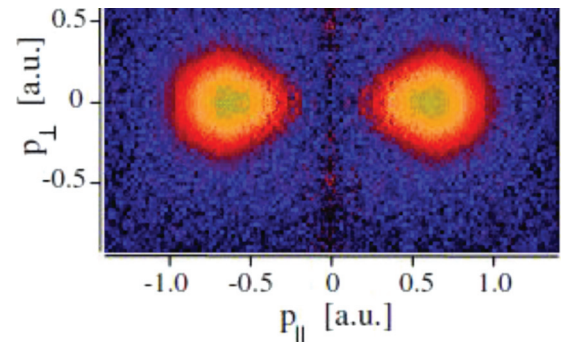


FIG. 5. (Color online) A momentum distribution measured by the Freiburg group [14] clearly shows the circular motion of a photoelectron produced by a circularly polarized laser beam. The propagation direction of the beam lies along the vertically oriented axis in the figure. The significance of this figure is discussed in Ref. [6].

(in Refs. [16,18], with some of the consequences explicated in Refs. [11,19]). The special nature of the ponderomotive potential is revealed in the present context of the Smeenk experiments through the result in Eq. (5): $p_{||} = U_p/c$. This is an expression of the effect of many photons acting collectively that replicates the energy-momentum connection of the single-photon expression $(\text{momentum})_{\text{photon}} = \hbar\omega/c$, $(\text{energy})_{\text{photon}} = \hbar\omega$, or $(\text{momentum})_{\text{photon}} = (\text{energy})_{\text{photon}}/c$. An important reminder is that, with circularly polarized light, all photon momenta are aligned parallel to the direction of propagation. This accounts for both the additive property of linear momenta as well as the already-mentioned additive property of angular momenta.

The analysis in the Smeenk paper leads to the conclusion that “. . . the ponderomotive energy does not transfer any net momentum to the electron.” This is in direct contradiction to the conclusions reached here. Smeenk assigns the value $2U_p/c$ to the forward momentum due to radiation pressure rather than U_p/c and then reduces this by an effect of the intensity gradient of the laser pulse. Despite the final agreement on the radiation pressure, this is still a major discrepancy in the physical interpretation. The problem can be localized to one sentence in the discussion above Eq. (1) in Smeenk: “To first order the electron velocity \mathbf{v} only depends on the electric field.” This cannot be correct, since it contradicts observed laboratory behavior. It is, however, inevitable in the length gauge, where the only preferred direction is the direction of the electric field vector. By contrast, the Coulomb gauge makes allowance for the three mutually perpendicular directions of the electric field, the magnetic field, and the propagation vector. Were it true that the “. . . electron velocity \mathbf{v} only depends on the electric field,” the photoelectron would emerge radially from the initial atom, whereas, as seen above, the photoelectron moves perpendicularly to the electric field as it follows its circular trajectory around the residual ion. This circular trajectory is a consequence of the requirement for angular momentum conservation. As pointed out above, angular momentum properties of individual photons can have major effects on the photoelectron, even while linear momentum effects are small.

The importance of U_p has some simple but basic consequences. As the Smeenk data show, the general conclusions reached here do not apply if the laser intensity is low. It must be true that ponderomotive effects dominate Coulomb effects from the residual ion in order for the arguments presented here to apply. As noted by T&D, this requires a large value for the z_1 intensity parameter, where

$$z_1 = 2U_p/E_B,$$

as defined in Ref. [20].

Basic properties of linearly polarized lasers can obviate the effects discussed here. Whereas photoionization by intense circularly polarized lasers gives rise to an energy spectrum that peaks at a kinetic energy approximately equal to U_p , the photoelectron spectrum from linearly polarized light reaches a peak at quite low energies. The most important part of the linear polarization spectrum arises from the absorption of relatively small numbers of photons, with a total transferred linear momentum contribution that might not be sufficient to overcome the attractive effects of the Coulomb interaction with

the residual ion. This can lead to negative values of $p_{||}$, as is true in the lowest intensity part of the Smeenk data, as well as being reported earlier [21].

VI. GAUGE DEPENDENCE OF PHYSICAL INTERPRETATIONS

It has been observed above that the length gauge analysis of Smeenk concludes that the ponderomotive energy makes no net contribution to the radiation pressure, whereas the diametrically opposite conclusion is reached here. There are (at least) two other analogous situations that are well known. One is the way that the ponderomotive potential enters into conservation conditions in atomic ionization. As viewed in the length gauge, the laser field needs to supply both the binding energy E_B and a dynamical Stark shift of the ionization edge in the amount U_p . In the velocity gauge or the Coulomb gauge, the laser must supply both E_B and the potential energy U_p of a charged particle immersed in a plane-wave field to achieve ionization of a bound electron. The threshold conditions are the same, but the physical meaning has changed radically.

A case of considerable historical importance began with the publication by Lamb [4] of a paper containing an appendix in which he calculated the line shape of the Lamb-shift transition. This required a second-order perturbation calculation in which it is necessary to carry out a sum over all intermediate states. This is difficult to do, but Lamb drew on his experience in the length gauge to know that he needed to consider only states close in energy to the initial and final states. He obtained thereby a plausible answer. However, he repeated the calculation in the velocity gauge and found an asymmetrical line shape that was in conflict both with the length gauge calculation and with laboratory observation. Lamb was disturbed by this seeming violation of gauge invariance, but succeeding authors seized on the Lamb result as evidence of an inherent superiority of the length gauge. The dilemma was resolved by Fried [5], who showed that, in the velocity gauge, all intermediate states are important, even states in the continuum. The two gauges were found to be equivalent after all, despite the major gauge-dependent difference in physical interpretations attributable to the relative contributions of intermediate states.

VII. OTHER IMPLICATIONS

A final remark is that the rescattering model [7,8] that has enjoyed wide popularity predicts that an electron ionized by circularly polarized light does not remain in the vicinity of the ion. Rather, it moves progressively farther away with each cycle of the field. The Smeenk measurements, the theory presented here, the Freiburg measurements reproduced in Fig. 5, and the U -matrix analysis of Ref. [15] all show that the photoelectrons enter a circular trajectory around the remnant ion. However, the classical equations of motion cited in the Corkum paper [7] do not allow any such trajectory. The only possibility is that a photoelectron will “walk away” from the ion (an expression employed by Corkum in talks on the subject) with no possibility of return. This “simple man” trajectory can be shown [18] to violate angular momentum and energy conservation, as well as experimental observation.

- [1] C. T. L. Smeenk, L. Arissian, B. Zhou, A. Mysyrowicz, D. M. Villeneuve, A. Staudte, and P. B. Corkum, *Phys. Rev. Lett.* **106**, 193002 (2011).
- [2] A. S. Titi and G. W. F. Drake, *Phys. Rev. A* **85**, 041404(R) (2012).
- [3] H. R. Reiss, *J. Opt. Soc. Am. B* **7**, 574 (1990).
- [4] W. E. Lamb, *Phys. Rev.* **85**, 259 (1952).
- [5] Z. Fried, *Phys. Rev. A* **8**, 2835 (1973).
- [6] H. R. Reiss, *Phys. Rev. A* **76**, 033404 (2007).
- [7] P. B. Corkum, *Phys. Rev. Lett.* **71**, 1994 (1993).
- [8] P. B. Corkum, *Phys. Today* **64**, 36 (2011).
- [9] H. R. Reiss, *Phys. Rev. A* **42**, 1476 (1990).
- [10] H. R. Reiss, *Prog. Quantum Electron.* **16**, 1 (1992).
- [11] H. R. Reiss, *Phys. Rev. Lett.* **101**, 043002 (2008); **101**, 159901(E) (2008).
- [12] H. R. Reiss, *Opt. Express* **8**, 99 (2001).
- [13] H. R. Reiss, in *Lectures on Ultrafast Intense Laser Science I*, edited by K. Yamanouchi (Springer, Berlin, 2010).
- [14] B. Bergues, Y. Ni, H. Helm, and I. Yu. Kiyan, *Phys. Rev. Lett.* **95**, 263002 (2005).
- [15] H. R. Reiss and N. Hatzilambrou, *J. Mod. Opt.* **53**, 221 (2006).
- [16] H. R. Reiss, *J. Mod. Opt.* **59**, 1371 (2012).
- [17] J. Schwinger, *Phys. Rev.* **82**, 664 (1951).
- [18] H. R. Reiss (unpublished).
- [19] H. R. Reiss, *Phys. Rev. Lett.* **102**, 143003 (2009).
- [20] H. R. Reiss, *Phys. Rev. A* **22**, 1786 (1980).
- [21] M. Førre, J. P. Hansen, L. Kocbach, S. Selstø, and L. B. Madsen, *Phys. Rev. Lett.* **97**, 043601 (2006).